Rare Metal Materials and Engineering
Volume 51, Issue 6, June 2022
Available online at www.rmme.ac.cn

Science Press

Cite this article as: Han Zhiyong, Wang Shicheng, Cheng Taotao, et al. Effect of Bonding Phases on Deposition Efficiency of YSZ-based Sealing Coating[J]. Rare Metal Materials and Engineering, 2022, 51(06): 1933-1941.

ARTICLE

Effect of Bonding Phases on Deposition Efficiency of YSZ-based Sealing Coating

Han Zhiyong[1], Wang Shicheng[1], Cheng Taotao[1,2], Xing Sijia[1], Wang Zhiping[1,2]

[1] Tianjin Key Laboratory for Civil Aircraft Airworthiness and Maintenance, Civil Aviation University of China, Tianjin 300300; [2] School of Mechanical Engineering, Hebei University of Technology, Tianjin 300401

Abstract: Four types of Y_2O_3 partially stabilized ZrO_2 (YSZ)-based agglomerated powder containing no bonding phase, Al_2O_3, yttrium aluminum garnet (YAG), and $MgAl_2O$, labeled as B0, B1, B2, and B3, respectively, were prepared by spray granulation. And, the flow ability, apparent density and particle size distribution of those powders were investigated. Besides, the deposition efficiency (DE) and bonding mechanism of the four types of agglomerated powder prepared by atmospheric plasma spraying (APS) were analyzed. The results show that, compared with B0 powder, the flowability of B1, B2 and B3 powder is reduced by 6.94%, 5.15% and 25.2%, respectively, the apparent density is reduced by 2.85%, 2.19% and 7.67%, respectively, and the proportion of large-size agglomerated powder is increased by 15.82%, 6.65% and 29.75%, respectively. The DE of B1, B2 and B3 powder is increased by 75.80%, 181.49% and 59.21%, respectively, and the main reason for the improvement of DE is the adhesion and wrapping effect of the bonding phase. Because YAG has the lowest melting point and moderate particle size, B2 powder has the best flowability, the maximum apparent density, and the smallest proportion of large particles, which accordingly results in the strongest adhesion and wrapping effect and eventually leads to the highest DE.

Key words: bonding phase; spray granulation; YSZ-based sealing coating; deposition efficiency

The application of sealing coating can minimize the gap between the stator and rotor, so as to significantly improve the efficiency of engines[1-4]. With increasing the gas temperature in turbine, metal-based sealing coating cannot meet the requirements of high temperature environment. Thereby, the ceramic-based sealing coating with higher service temperature (above 1000 °C) has attracted much research interest[5-8].

Most studies in the field of ceramic-based sealing coating focus on the improvement of its performance, such as thermal aging, thermal cycling, corrosion, abradability. However, the deposition efficiency (DE) of ceramic-based sealing coating is very low, generally about 10%~15%, which is far lower than the average of 30%~50% of thermal spraying coatings. Such low DE obviously leads to serious waste of materials and increase of the manufacturing costs, and thus restricts the practical application of the ceramic-based sealing coating. The reasons for the low DE can be summarized as follows. (1) The melting point of ceramics is extremely high, i.e., melting point of Y_2O_3 partially stabilized ZrO_2 (YSZ) reaches about 2700 °C, while the residence time of ceramics particles in the plasma jet is only about 10^{-4}~10^{-5} s. Due to the high melting point and the extremely short heating time, the ceramic powder is difficult to be fully melted, which significantly reduces the DE. (2) The time interval between two neighboring particles colliding with the substrate is much longer than the time required for complete solidification of the particles after spreading[9]. As a result, the deposited ceramic layers already become solid state when it is impacted by the subsequent particles. The ceramics feature high hardness and brittleness, and the toughness is basically zero. If the particles in the plasma jet are not melted or semi melted, they cannot be embedded in the already-deposited ceramic layer when they impact the solid ceramic layer. Meanwhile, it is also hard to combine with the already-deposited ceramic layer by the anchoring effect due to the plastic deformation of the particles themselves. (3) For ceramic-based sealing coating, poly-p-

Received date: June 15, 2021
Foundation item: Natural Science Research Project of Tianjin Education Commission (2020KJ030); Fundamental Research Funds for the Central Universities (3122020057)
Corresponding author: Cheng Taotao, Candidate for Ph.D., Tianjin Key Laboratory for Civil Aircraft Airworthiness and Maintenance, Civil Aviation University of China, Tianjin 300300, P. R. China, Tel: 0086-22-24092514, E-mail: cheng604@126.com

hydroxybenzoate (PHB) is added to YSZ powder as the pore-forming agent. The thermal stability temperature of PHB is lower than 300 °C, which makes it easy to burn during the atmospheric plasma spraying (APS) process.

Optimization of the spraying process is the common method to improve the DE of APS ceramic coatings. Wang et al[10] found that increasing the spraying power and reducing the powder feeding rate can effectively improve the DE of the lanthanum zirconate ceramic coating, but causes negative effects on the bonding strength and thermal shock resistance. Wang et al[11] studied the effect of APS process parameters on the DE of Al_2O_3-40wt% TiO_2 coating. The results demonstrated that the DE is closely dependent on the spray current and voltage. According to the research of Bobzin et al[12], larger particles which penetrate into the center of the plasma jet features higher speed and temperature, which results in higher DE than particles on the jet periphery. In recent years, adding low melting point components to raw materials becomes an attractive method to improve DE. Zhao et al[13] added low-melting MoO_3 powder to the nickel-based composite coating fabricated by laser cladding and achieved increase of the DE of laser cladding. Yang et al[14] used metallic Ni as the bonding phase to fuse together with other components and prevent them from blowing off during APS process, thereby increasing the DE of the coating. However, there are few researches on the improvement of DE of APS ceramic-based sealing coatings by adding low-melting ceramic phases.

In this work, Al_2O_3, yttrium aluminum garnet (YAG) and $MgAl_2O_4$ were selected as three high temperature bonding phases and added to YSZ-based powders. The effects of different bonding phases on the flow ability, apparent density and particle size distribution of the four types of agglomerated powder were investigated. In addition, the effects of different bonding phases on the DE by APS were investigated. Moreover, bonding mechanisms of the different bonding phases were clarified.

1 Experiment

1.1 Main components of agglomerated particles

YSZ ceramic material is the base phase of YSZ-based agglomerated powder, which provides high-strength ceramic framework and excellent thermo physical properties. Its melting point is about 2700 °C.

As shown in Fig. 1, YSZ raw powder used in this work features a particle size of about 1 μm and is irregularly granular, which was provided by Shanghai Shuitian Material Technology Co., Ltd.

The melting point of Al_2O_3 is 2054 °C, which is 23.93% lower than that of YSZ. Al_2O_3 is one of the commonly-used high temperature resistant materials. According to Ref. [15, 16], Al_2O_3 coating has the potential as a high temperature sealing coating. Hence, Al_2O_3 was selected as a high-temperature bonding phase in YSZ-based high temperature sealing coating in this work. As shown in Fig.2, the used Al_2O_3 particles are about 1 μm in particle size and irregularly granular, which was provided by Shanghai Shuitian Material Technology Co., Ltd.

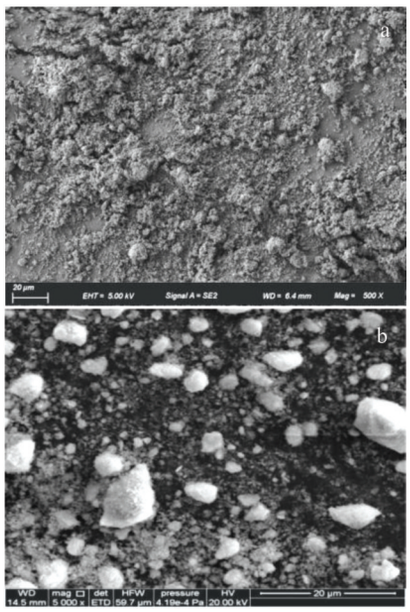

Fig.1 Micro morphologies of YSZ raw powder

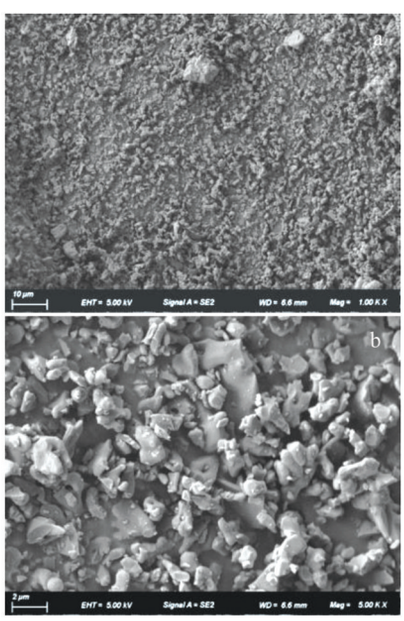

Fig.2 Micromorphologies of the Al_2O_3 raw powder

The melting point of YAG is 1950 °C, which is 27.78% lower than that of YSZ. YAG has excellent phase stability and thermal stability, thereby becoming a next-generation high temperature resistant coating material[17,18]. YAG was selected in this work as the second high-temperature bonding phase in YSZ-based high-temperature sealing coating. The used YAG raw powder was purchased from Shanghai Paddy Material Technology Co., Ltd. As shown in Fig. 3, the YAG powder used in this work features a particle size of about 10 μm and irregular block shape.

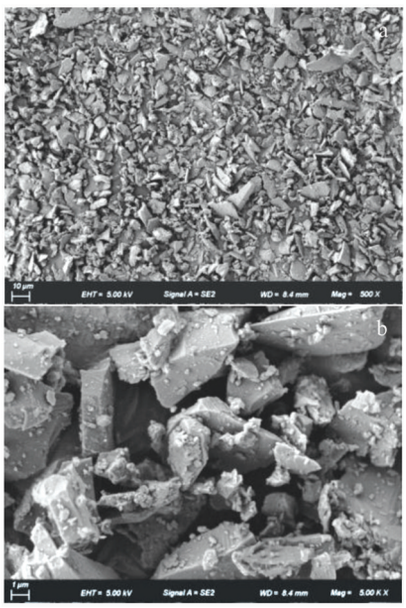

Fig.3 Micromorphologies of the YAG raw powder

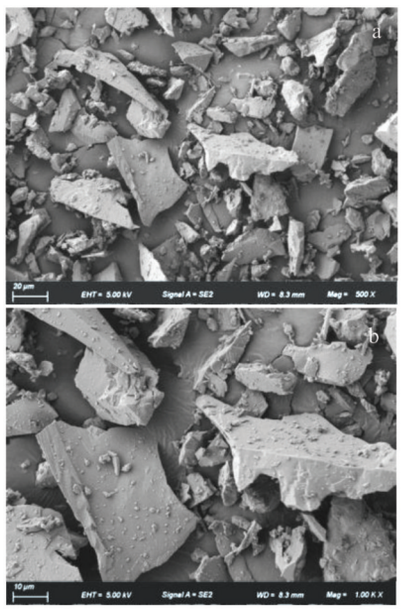

Fig.4 Micromorphologies of $MgAl_2O_4$ raw powder

The melting point of $MgAl_2O_4$ is 2250 °C, which is 16.67% lower than that of YSZ. $MgAl_2O_4$ is a synthetic spinel refractory material and the working temperature of the $MgAl_2O_4$ sealing coating has the potential to beyond 1400 ° C[19,20]. $MgAl_2O_4$ was selected in this work as the third high-temperature bonding phase in YSZ-based high temperature sealing coating. The used $MgAl_2O_4$ raw powder was purchased from Gongyi Sanhe Refractory Co., Ltd. As shown in Fig. 4, the used $MgAl_2O_4$ powder features a particle size of about 20 μm and irregular block shape.

PHB is commonly-used in thermal spray sealing coatings as the low-temperature lubricating phase and high-temperature pore-forming phase. The PHB used in this work was purchased from Zhonghao Chenguang Chemical Research Institute Co., Ltd. Fig. 5 shows the micromorphologies of PHB. The used PHB is in the form of irregular agglomerated particles with a particle size of about 20 μm.

1.2 Auxiliary materials for spray granulation

The dispersants and adhesives used in the spray granulation process are shown in Table 1.

1.3 Components of slurry suspension

The four types of agglomerated powder with no bonding phase, Al_2O_3, YAG and $MgAl_2O_4$ were labeled as B0, B1, B2 and B3 powder, respectively. Table 2 shows the contents of components of the slurry suspension during the spray granulation of the four types of agglomerated powder.

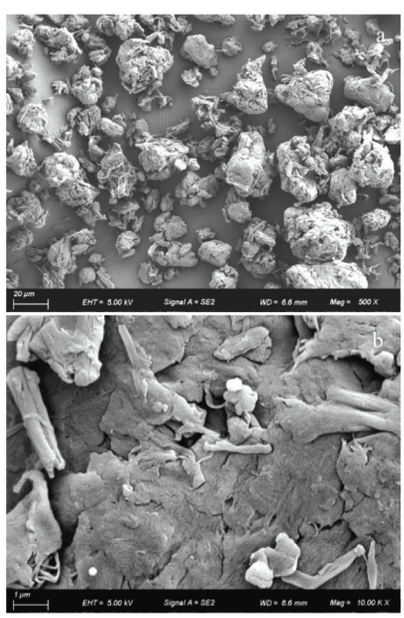

Fig.5 Micromorphologies of PHB raw powder

1.4 Methods

The raw materials were crushed and mixed uniformly by planetary ball mill. YSZ-based agglomerated powders containing different bonding phases were prepared by spray granulation. The fluidity of agglomerated powder was measured with a Hall flow meter according to GB/T 1482-

Table 1 Dispersants and adhesives

Material	Manufacturer	Purity	Function
Sodium hexametaphosphate	Shandong Yousuo Chemical Technology Co., Ltd	Analytically pure	Dispersant
PEG (Polyethylene glycol)	Wuxi Yatai United Chemical Co., Ltd	Analytically pure	Dispersant
PVA (polyvinyl alcohol)	Shanghai Yingjia Industrial Development Co., Ltd	≥97.0%	Adhesive

Table 2 Contents of components in slurry suspension (g)

Material	Component content			
	B0	B1	B2	B3
PHB	20	20	20	20
YSZ	180	180	180	180
Sodium hexametaphosphate	4	4	4	4
PEG	20	20	20	20
PVA	10	10	10	10
Al_2O_3	0	40	0	0
YAG	0	0	40	0
$MgAl_2O_4$	0	0	0	40
Deionized water	230	270	270	270

2010. The apparent density of agglomerated powder was measured by the funnel method according to GB/T 1479.1-2011. The particle size range of agglomerated powder was measured by standard sieves according to GB/T 21524-2008. The four types of agglomerated powders were sprayed by APS and characterized by scanning electron microscope (SEM) and energy dispersive spectrometer (EDS). The DE of four types of agglomerated powders was measured through the mass ratio of the coating deposited to powder consumed [21].

2 Performance of Agglomerated Powder

2.1 Micromorphology

Fig.6 shows the micromorphologies of B0, B1, B2 and B3 agglomerated powder. The four types of agglomerated powders are spherical. Al_2O_3 particles, YAG particles and $MgAl_2O_4$ particles are uniformly distributed in B1, B2 and B3 agglomerated powder, respectively.

2.2 Flowability and apparent density

Excellent flowability and apparent density are necessary for APS of agglomerated particles. Furthermore, they also play an important role in realizing good performance of coating. The results of flowability and apparent density of B0, B1, B2 and B3 agglomerated powder are shown in Fig.7.

In the flowability testing experiments as introduced in Sec. 1.4, longer flowing time means worse flowability. As shown in Fig.7, B0 powder features the best flowability with a flowing time of 89.3 s/50 g. The flowing time of B1 B2 and B3 powder is increased by 6.94%, 5.15% and 25.2%, respectively, compared to that of B0 powder. Accordingly, the flowability level of B1 and B2 powder is almost the same, which is only slightly decreased compared with B0 powder. However, the flowability of B3 powder is the worst, which is significantly decreased compared with other types of powder. The apparent density of B0 powder is the largest and the apparent density of B1, B2 and B3 powder is decreased by 2.85%, 2.19% and 7.67%, respectively.

2.3 Particle size distribution

Particle size distribution of agglomerated particles directly affects the heat conduction and melting degree in the plasma jet. The particle sizes of B0, B1, B2, and B3 agglomerated powder are shown in Table 3. Fig. 8 is the particle size distribution diagram of the four types of agglomerated powder, which is close to the normal distribution, consistent with the test result in Ref.[22]. In the range of 38~150 μm and 53~150 μm, the particle size distribution levels of B0, B1, B2 and B3 agglomerated powders are almost the same. However, the distribution levels of B0, B1, B2 and B3 agglomerated powder in the particle size range of 75~150 μm (large particle) are quite different, which are 41.34%, 47.88%, 44.09% and 53.64%, respectively. Compared with B0 powder, the proportions of large particle in B1, B2 and B3 agglomerated powder are increased by 15.82%, 6.65% and 29.75%, respectively.

3 DE and Deposition Mechanism

3.1 DE of four types of agglomerated powder

Table 4 shows the DE of four types of agglomerated powder sprayed by APS. Compared with B0 powder, the DE of B1, B2 and B3 agglomerated powder are increased by 75.80%, 181.49% and 59.21%, respectively. Specifically, the

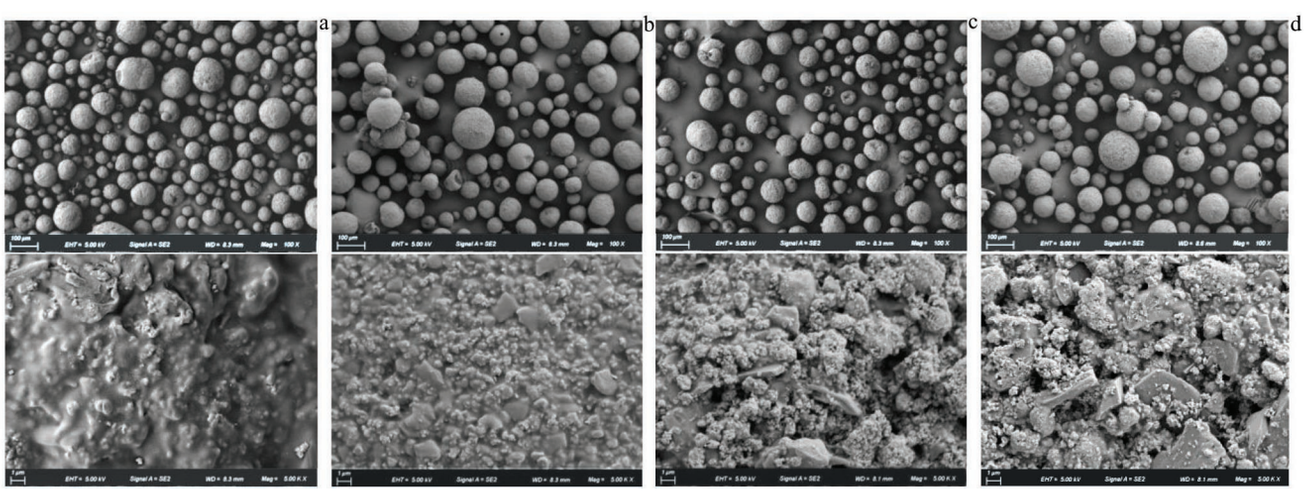

Fig.6 Micro morphologies of four types of agglomerated powder: (a) B0, (b) B1, (c) B2, and (d) B3

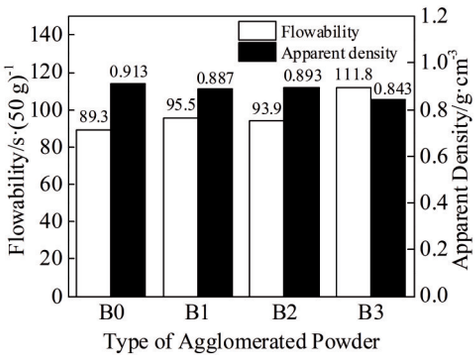

Fig.7 Flowability and apparent density of four types of agglomerated powder

Table 3 Particle size distribution of four types of agglomerated powder

Agglomerated powder	Proportion of powder passing standard sieve/wt%			
	100# (150 μm)	200# (75 μm)	325# (53 μm)	400# (38 μm)
B0	100	58.66	11.28	3.76
B1	100	52.12	10.40	3.85
B2	100	55.91	11.01	3.54
B3	100	46.36	10.48	4.28

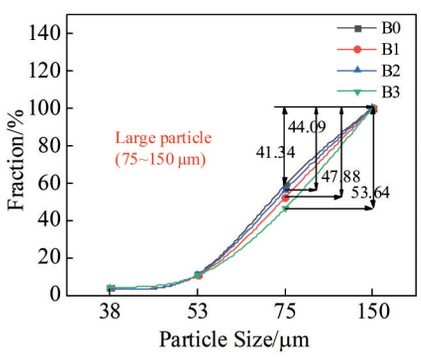

Fig.8 Particle size distribution of four types of agglomerated powders

Table 4 DE of four types of agglomerated powder (%)

Powder	Sample 1	Sample 2	Sample 3	Average
B0	12.21	9.36	9.55	10.37
B1	21.74	15.30	17.66	18.23
B2	14.98	16.51	18.05	16.51
B3	27.54	30.36	29.68	29.19

B2 agglomerated powder with YAG bonding phase is significantly improved.

3.2 Spreading morphology of four types of agglomerated powder

In order to analyze the effect of bonding phases on DE, the spreading morphology of B0, B1, B2 and B3 agglomerated powder was observed by SEM, as shown in Fig.9. As shown in Fig.9a, the molten B0 powder mainly exhibits irregular and small lamellas after impacting on the substrate. The surface of the lamellas is very smooth, indicating that there are almost no other unmelted or unburned particles on it. Compared with B0 powder, the spreading morphologies of B1, B2 and B3 powder all show larger lamellas and the lamellas are adhered or wrapped with varying content of unmelted and unburned particles. The content of unmelted and unburned particles adhered or wrapped in B2 lamellas is the highest, followed by B1 lamellas and B3 lamellas.

3.3 Analysis of deposition mechanism

For B0 agglomerated powder without bonding phase, due to the high melting point of YSZ particles and the short residence time in the plasma jet, only part of YSZ particles can be heated to molten state. This results in a fact that only a small amount of molten YSZ droplets can effectively spread and deposit on the substrate, which eventually leads to the lowest DE during APS with B0 powder.

For B1, B2 and B3 agglomerated powder, three types of agglomerated powders contain low temperature bonding phases, i. e., Al_2O_3, YAG and $MgAl_2O_4$, which are easier to reach molten state in the plasma jet. The molten low temperature bonding phases have adhesion and wrapping effect on the unmelted and unburned particles in the subsequent impacting and spreading process. Thus, the DE of the three types of agglomerated powder is all improved compared with that of B0 agglomerated powder. However, it should be noticed that different molten low temperature bonding phases feature different adhesion and wrapping effects, which results in different improved DE during APS with the three types of agglomerated powder.

In order to further analyze the adhesion and wrapping mechanism of different bonding phases, EDS was carried out on the typical areas of B1, B2 and B3 spreading lamellas.

Fig. 10 shows the micromorphologies and EDS spectra of B1 spreading laminas. There are medium content of granular and spherical adhesive particles on the B1 lamellas. As shown in Fig. 10a, the adhesive area of B1 lamellas mainly contains C, O, Al and Zr elements, and considering the main components of B1 agglomerated powder, the main phases contained in the adhesive area are YSZ, Al_2O_3 and PHB. As shown in Fig.10b, the granular particles of B1 lamellas mainly contain O and Zr elements, indicating that the main phase in the granular particles is YSZ. As shown in Fig. 10c, the spherical particles of B1 lamellas mainly contain O, Al and Zr elements. Considering the small particle size and low melting point of Al_2O_3 raw material, the spherical particles are mainly YSZ particles wrapped by molten Al_2O_3 materials.

Fig. 11 shows the micromorphologies and EDS spectra of B2 spreading laminas. The content of adhesion or wrapping materials on the surface of B2 laminas is the most, in addition to a large number of granular adherents. There are also obvious wrapping areas in the B2 lamellaes. As shown in Fig. 11a, the adhesive area of B2 lamellas mainly contains O and Zr elements, indicating that the main phase in the

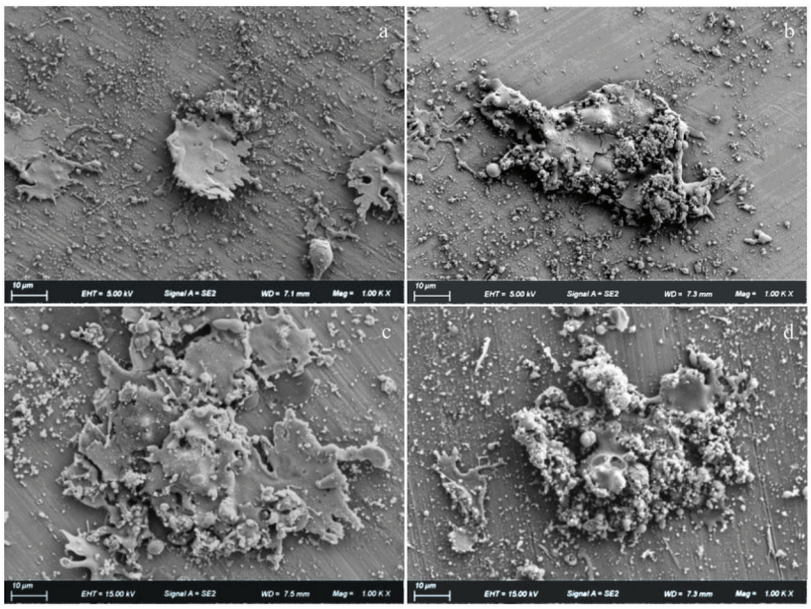

Fig.9 Spreading morphologies of four types of agglomerated powders: (a) B0, (b) B1, (c) B2, and (d) B3

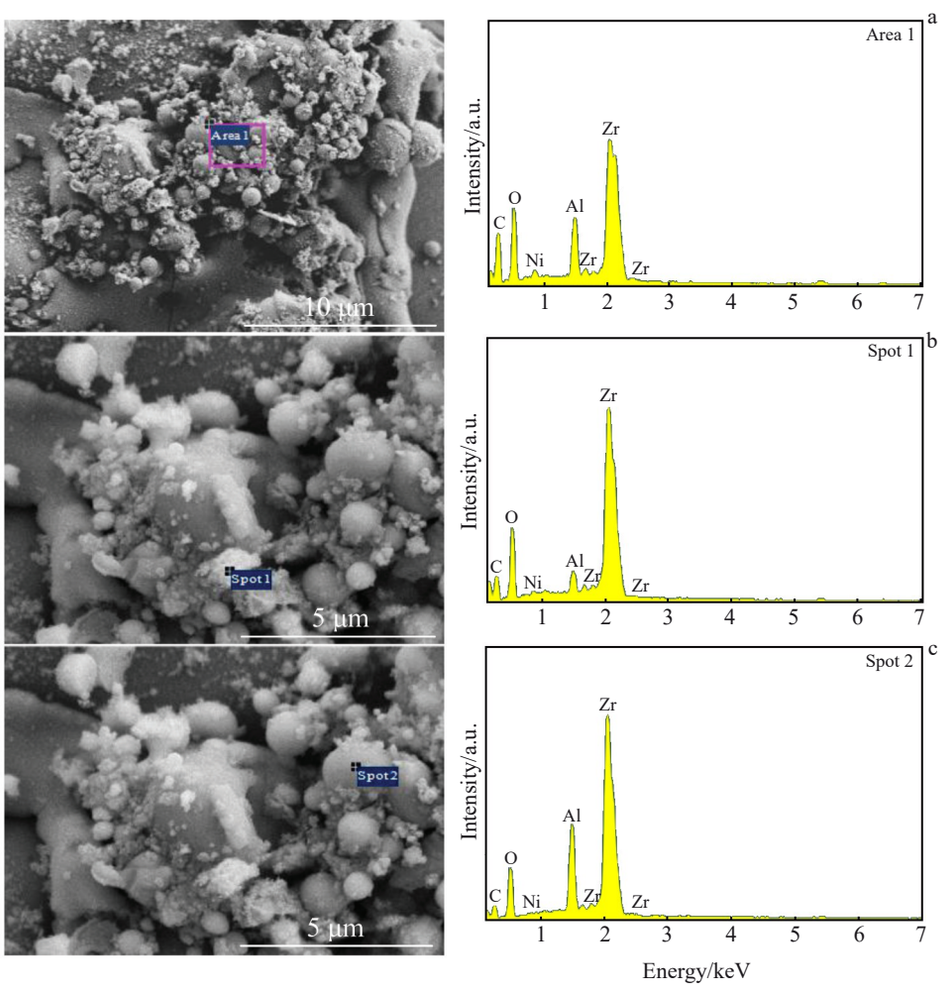

Fig.10 Micromorphologies and EDS spectra of B1 lamellas: (a) adhesion area, (b) granular particle, and (c) spherical particle

adhesive area is YSZ. As shown in Fig.11b, the wrapping area of B2 lamellas mainly contains Y, Al, O and Zr elements. Considering the main components of B2 agglomerated powder, the main phases in the wrapping area are YAG and

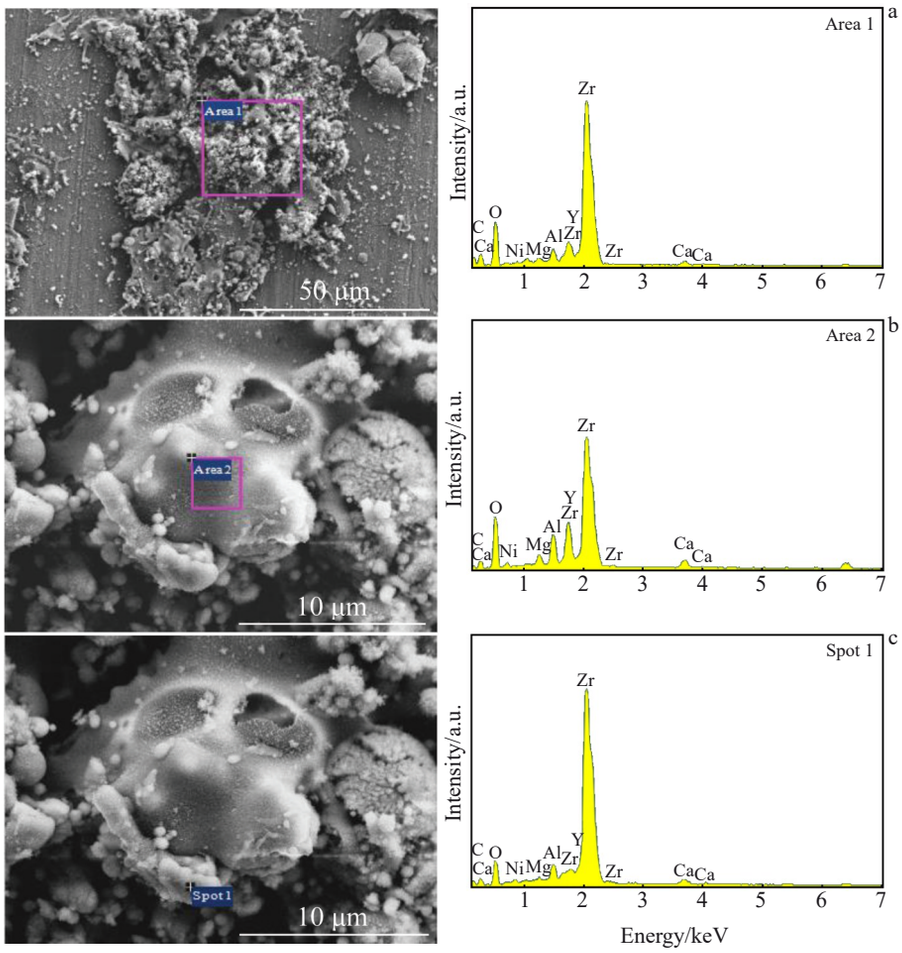

Fig.11 Micromorphologies and EDS spectra of B2 lamellas: (a) adhesion area, (b) wrapping area, and (c) adhesive particles

YSZ. As shown in Fig. 11c, the adhesive particles of B2 lamellas mainly contain O and Zr elements. Therefore, the adhesive particles are mainly YSZ particles.

Fig. 12 shows the micromorphologies and EDS spectra of the B3 spreading laminas. The content of adhesion or wrapping materials on the surface of B3 laminas is the least, while the B3 laminas are mainly composed of wrapping area and adhesion area. As shown in Fig.12a, the wrapping area of B3 lamellas mainly contains O, Al and Zr elements. Considering the main components of B3 agglomerated powder, the main phases in the wrapping area are YSZ and $MgAl_2O_4$. As shown in Fig. 12b, the adhesion area of B3 lamellas mainly contains O, Al and Zr elements. However, it should be noted that compared with the EDS results of the wrapping area in Fig. 12a, the peak intensity of Al element is significantly enhanced. Therefore, the adhesion area is composed of a small amount of YSZ particles adhered to the molten $MgAl_2O_4$ materials. As shown in Fig.12c, the adhesive particles of B3 lamellas mainly contain O, Al and Zr elements. It should also be noted that compared with the EDS results of the adhesion area in Fig.12b, the peak intensity of Al element is significantly reduced. Thus, the adhesive particles are mainly YSZ.

Based on abovementioned experimental results, it is clear that the effects of Al_2O_3, YAG and $MgAl_2O_4$ on the deposition behavior of the three types of agglomerated powder are mainly manifested in two aspects. On the one hand, the bonding phases have a adhesion effect on the unmelted YSZ and unburned PHB particles. For B1 powder containing Al_2O_3 bonding phase, the melting point of Al_2O_3 is relatively low. The flowability, apparent density and proportion of large particles of the powder are moderate. Hence, Al_2O_3 is able to reach molten state relatively easily in the plasma jet, which leads to a good adhesion effect and can form the granular adhesion area, as shown in Fig.10b. For B2 powder containing YAG bonding phase, due to the lowest melting point of YAG, the best flowability, the largest apparent density and the smallest proportion of large particles of the powder, YAG is able to reach the molten state most easily, which leads to the strongest adhesion effect and forms the largest content of adhesion or wrapping materials, as shown in Fig. 11a. For B3 powder containing $MgAl_2O_4$ bonding phase, due to the highest melting point of $MgAl_2O_4$, the worst flowability, the smallest apparent density and the largest proportion of large particles of the powder, it is relatively difficult for $MgAl_2O_4$ to reach the molten state, which leads to the worst adhesion effect.

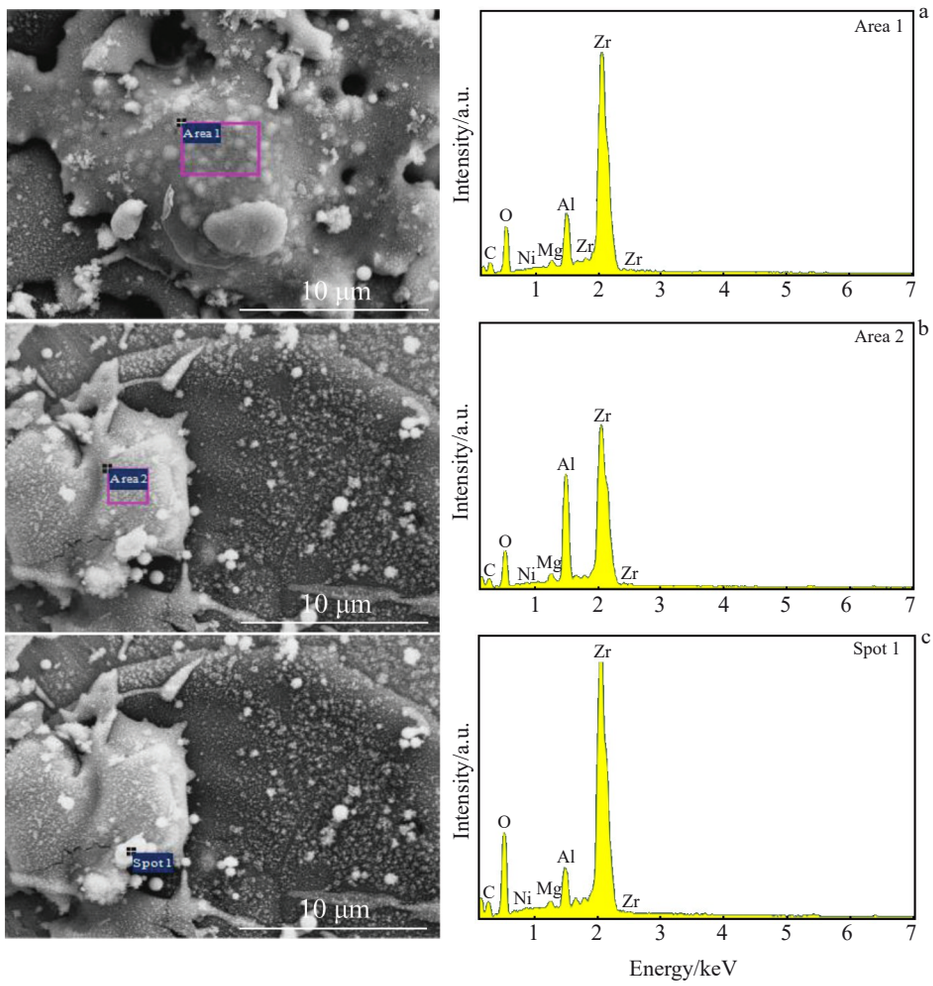

Fig.12 Micromorphologies and EDS spectra of B3 lamellas: (a) wrapping area, (b) adhesion area, and (c) adhesive particles

Thereby, $MgAl_2O_4$ can only adhere few and small YSZ particles, as shown in Fig. 12b and 12c. On the other hand, bonding phases have a wrapping effect on unmelted YSZ and unburned PHB particles. Although the molten state of Al_2O_3 is relatively good, the particle size of Al_2O_3 is too small. This leads to the fact that partially melted Al_2O_3 particles are directly coated on the surface of YSZ particles and form spherical particles, as shown in Fig. 10c. The molten state of YAG is the best and the particle size of YAG is moderate, so that the wrapping effect of YAG is the strongest that causes the wrapping area, as shown in Fig. 11b. The molten state of $MgAl_2O_4$ is the worst, and the particle size of $MgAl_2O_4$ is too large, which results in relatively bad wrapping effect of $MgAl_2O_4$. As a result, $MgAl_2O_4$ can only wrap few and small YSZ particles, as shown in Fig.12a.

4 Conclusions

1) B0 agglomerated powder is featured with the highest flowability, the largest apparent density and the smallest proportion of large particle among the four different agglomerated powder, i. e., B0, B1, B2, and B3. Compared with B0 agglomerated powder, the flowability of B1, B2 and B3 agglomerated powder is decreased by 6.94%, 5.15% and 25.2%; the apparent density of B1, B2 and B3 is decreased by 2.85%, 2.19% and 7.67%; the proportion of large particle agglomerated powder is increased by 15.82%, 6.65% and 29.75%, respectively.

2) Compared with B0 agglomerated powder, the deposition efficiency (DE) of B1, B2 and B3 agglomerated powder is increased by 75.80%, 181.49% and 59.21%, respectively. The main reason for the improvement of DE is that the three types of bonding phases have adhesion and wrapping effects on the unmelted YSZ particles and unburned PHB particles. Additionally, the different adhesion and wrapping effects of the three agglomerated powders lead to different DE. Due to the lowest melting point and the moderate particle size of YAG raw powder, B2 agglomerated powder is featured with the best flowability, the largest apparent density and the smallest proportion of large particles, which accordingly result in the strongest adhesion and wrapping effect and eventually lead to the highest DE.

References

1 Sporer D, Wilson S, Dorfman M. *Ceramic Engineering and Science Proceedings*[J], 2010, 30(3): 39

2 Chen Lingyun. *Thesis for Doctorate*[D]. Beijing: University of Science and Technology Beijing, 2018
3 Tang Zhihui, Guo Mengqiu, Zhou Zimin *et al. China Surface Engineering*[J], 2019, 32(1): 78
4 Wang Zhe, Du Lingzhong, Lan Hao *et al. Ceramics International* [J], 2019, 45(9): 11 802
5 Sun X M, Du L Z, Lan H *et al. Surface & Coatings Technology* [J], 2020, 397: 126 045
6 Cui Yongjing, Guo Mengqiu, Wang Changliang *et al. Surface & Coatings Technology*[J], 2020, 394: 125 915
7 Jech D, Remešová M, Komarov P *et al. Solid State Phenomena* [J], 2019, 296: 161
8 Ding Kunying, Cheng Taotao, Han Zhiyong. *Rare Metal Materials and Engineering*[J], 2018, 47(6): 1677
9 Zhao Qin. *Thesis for Master*[D]. Tianjin: Hebei University of Technology, 2018
10 Wang Jing, Bai Shuxin, Li Shun *et al. Heat Treatment of Metals* [J], 2010, 35(4): 24
11 Wang Y J, Xu J Y, Zhao Q H *et al. IOP Conference Series: Materials Science and Engineering*[J], 2017, 213(1): 12 042
12 Bobzin K, Wietheger W, Heinemann H *et al. Surface & Coatings Technology*[J], 2020, 399: 126 118
13 Zhao Yue, Feng Kai, Shen Chen *et al. Materials Letters*[J], 2019, 257: 126 614
14 Yang Qionglian. *Thesis for Master*[D]. Kunming: Kunming University of Science and Technology, 2019
15 Gao Junguo, Lu Feng, Guo Mengqiu. *Advanced Materials Research*[J], 2014, 3643: 274
16 Li Changjiu, Zou Jiao, Huo Huibin *et al. Journal of Thermal Spray Technology*[J], 2016, 25(1-2): 264
17 Musalek R, Tesar T, Medricky J *et al. Journal of Thermal Spray Technology*[J], 2021, 30: 81
18 Li Wensheng, Zhang Yi, An Guosheng *et al. Rare Metal Materials and Engineering*[J], 2019, 48(12): 3961 (in Chinese)
19 Steinke T, Mauer G, Vassen R *et al. Journal of Thermal Spray Technology*[J], 2010, 19(4): 756
20 Ebert S, Mücke R, Mack D *et al. Journal of the European Ceramic Society*[J], 2013, 33(15-16): 3335
21 Peng Ruzhen, Li Rongxing, Yu Xiaohua *et al. Heat Treatment of Metals*[J], 2016, 41(3): 37
22 Gong Zijian. *Thesis for Doctorate*[D]. Harbin: Harbin Institute of Technology, 2016

粘接相对YSZ基高温封严涂层沉积效率的影响

韩志勇[1]，王仕成[1]，程涛涛[1,2]，邢思佳[1]，王志平[1,2]
(1. 中国民航大学 天津市民用航空器适航与维修重点实验室，天津 300300)
(2. 河北工业大学 机械工程学院，天津 300401)

摘　要：通过喷雾造粒法制备出含不同粘接相的B0（不含粘接相）、B1（氧化铝）、B2（钇铝石榴石）和B3（镁铝尖晶石）4种YSZ（Y_2O_3 partially stabilized ZrO_2）基团聚颗粒，对4种团聚颗粒的流动性、松装密度及粒径分布进行了研究。利用等离子喷涂技术制备了上述4组高温封严涂层，测量了各组粉末的沉积效率，分析了不同粘接相的粘接机理。结果表明，与B0型团聚粉末相比，B1、B2和B3型团聚粉末的流动性分别降低了6.94%、5.15%和25.2%，松装密度分别减少了2.85%、2.19%和7.67%，大粒度的团聚粉末所占比例分别提高了15.82%、6.65%和29.75%；B1、B2和B3型团聚粉末的沉积效率分别提高了75.80%，181.49%和59.21%。粘接相熔融后对未熔融YSZ粒子和未烧损聚苯酯粒子的黏附和包裹作用是提高涂层沉积效率的主要原因。由于钇铝石榴石粘接相熔点最低、粒度适中，得到的B2型团聚颗粒流动性最好，松装密度最大，大颗粒所占比例最小，因此B2型涂层具有最高的沉积效率。

关键词：粘接相；喷雾造粒；YSZ基封严涂层；沉积效率

作者简介：韩志勇，男，1970年生，教授，中国民航大学天津市民用航空器适航与维修重点实验室，天津 300300，电话：022-24092514，E-mail：zyhan@cauc.edu.cn